#No 2040
LBL
16.9.36
2040

Pressure Drop and Flow Characteristics of Short Capillary Tubes at Low Reynolds Numbers[1]

By FRANK KREITH[2] and RAYMOND EISENSTADT[3]

The pressure drop and flow characteristics of short capillary tubes have been investigated experimentally for length-to-diameter ratios varying from 0.45 to 18 at diameter Reynolds numbers ranging from 8 to 1500. In the range of the dimensionless modulus $(L\mu)/(VD^2\rho)$ from 4×10^{-3} to 3 to 10^{-1}, the experimental data agree within 15 per cent with a mathematical theory by Langhaar (1).[4] At a value of $(L\mu)/(VD^2\rho)$ of about 0.3 the experimental data approach the Poiseuille laminar-flow theory (2). For very short tubes ($L/D < 0.5$) the experimental results deviate from Langhaar's theory at values of $L\mu/VD^2\rho$ less than 4×10^{-3}, and at $L\mu/VD^2\rho$ equal to 5×10^{-4}, the pressure drop is twice as large as that predicted by Langhaar's theory (1). The experimental results for tubes having very short aspect ratios are in agreement with data obtained by Zucrow (12) with short square-edged jets. It was found that the flow rate $\dot{Q}$ through a short capillary tube can be related empirically to the over-all pressure drop $\overline{\Delta p}$ raised to a power N. The exponent N is a function of the length-to-diameter ratio L/D varying from 0.5 at L/D equal to 0.45 to 0.91 at L/D of 18. The trend of the curve suggests an asymptotic approach to unity, the exponent for Poiseuille-type flow. The results of this study have application to: (a) Simulating flow through screens, doors, cracks, and fissures in small-scale model testing of buildings in atmospheric wind tunnels. (b) Automatic control devices where capillary tubes are used as hydraulic resistances in a larger line and in nozzle-flapper combinations. (c) Heat pumps and air-conditioning equipment where short capillary tubes are used as two-way control valves. (d) Flow through compact heat exchangers and porous materials.

Nomenclature

The following nomenclature is used in the paper:

C = orifice coefficient, defined by Equation [10]
D = diameter of tube, in.
g_c = 32.2 ft-lb$_M$/lb$_F$ — sec^2
$\bar{f}_{APP}$ = integrated apparent friction coefficient, defined by Equation [8]
k = characteristic flow exponent, defined by Equation [1]
L = length of tube, in.
N = characteristic pressure-drop exponent, $1/2k$
p = static pressure, psf
Δp = static pressure drop, psf
$\overline{\Delta p}$ = total pressure difference between reservoirs connected by capillary tubes, psf or in. H_2O
$\dot{Q}$ = volumetric flow rate, cfm
V = mean velocity, $9.6\,\dot{Q}/\pi D^2$, fps
x = distance from the inlet section, illustrated in Fig. 4.
Re_D = Reynolds number, $0.8\dot{Q}\rho/\pi D\mu$, dimensionless
μ = dynamic viscosity, lb$_M$/ft-sec
ρ = mass density, lb$_M$/ft^3

Introduction

It is usual to express the pressure drop of an incompressible fluid flowing through a duct or an orifice as a function of velocity by a relation of the type

$$\frac{\Delta p}{\rho} = 4\bar{f}_{APP}\frac{L}{D}\left(\frac{V^2}{2g_c}\right) \simeq \text{const}\left(\frac{V^2}{2}\right)^k \quad [1]$$

where the exponent k in Equation [1] depends upon the flow system. For some common flow systems Equation [1] yields the following relations between pressure loss and velocity:

1 Orifices, screens, or grids (above critical Reynolds number, $\bar{f}_{APP}$ = const)

$$\Delta p \sim V^2,\ k = 1 \quad [2]$$

2 Turbulent flow in ducts ($\bar{f}_{APP} = \text{const}/Re_D^{0.2}$)

$$\Delta p \sim V^{1.8},\ k = 0.9 \quad [3]$$

3 Fully developed laminar flow in ducts ($\bar{f}_{APP} = \text{const}/Re_D$)

$$\Delta p \sim V,\ k = 0.5 \quad [4]$$

While numerous investigations have been made to determine the flow characteristics of the foregoing systems in fully developed laminar and turbulent flow, the data available for laminar flow in short tubes are scant and inconclusive. A survey of available experimental data and analytical investigations on laminar flow in the inlet zone of ducts (2 to 7) is contained in reference (8).

The interest in this flow regime arose originally as a result of the need to simulate various types of flow through screens, doors, windows, and the like, in tests of small-scale models of buildings in an atmospheric type of wind tunnel.

It is well known that the pressure drop of a fluid under laminar-flow conditions in short tubes is considerably larger than the value predicted from the Poiseuille law. This is a result of the changes in the velocity profile occurring near the tube entrance. When a fluid enters a duct, the fluid particles adjacent to the

[1] This paper reports work done under contract with the Chemical Corps, U. S. Army, Washington, D. C.
[2] Associate Professor of Mechanical Engineering, Lehigh University, Bethlehem, Pa. Assoc. Mem. ASME.
[3] Assistant Professor, Department of Mechanical Engineering, Union College, Schenectady, N. Y.; formerly, Assistant Professor of Civil Engineering, Lehigh University. Assoc. Mem. ASME.
[4] Numbers in parentheses refer to the Bibliography at the end of the paper.
Contributed by the Hydraulic Division and presented at the Semi-Annual Meeting, Cleveland, Ohio, June 17–21, 1956, of The American Society of Mechanical Engineers.
Note: Statements and opinions advanced in papers are to be understood as individual expressions of their authors and not those of the Society. Manuscript received at ASME Headquarters, January 17, 1956. Paper No. 56—SA-15.

ASME TRANS Vol 79 pp 1070-1078 Report No 56-SA-15, 01:07:1957

wall are slowed down by the viscous forces while the particles in the inner core are not directly affected by these forces for some distance from the entrance. Under the influence of the frictional forces the thickness of the retarded fluid layer grows. Since the mass-flow rate remains constant, it is necessary for the fluid in the inner core to speed up until finally a parabolic velocity distribution is reached some distance from the entrance. The change in momentum of the fluid in the inner core can only be produced by a force over and above that which is required to overcome the friction between the fluid and the pipe wall. This force shows up as an increase in the pressure difference required to move a given quantity of fluid through a short tube.

The superposition of the pressure drop resulting from the momentum change upon the pressure drop caused by the tractive forces at the wall of a duct offers the possibility of obtaining various values of the exponent k in Equation [1] by a proper balance between the two mechanisms. Thus, by a proper selection of the length-to-diameter ratio, it is possible to simulate various types of flow system, even if the reduction in scale of the prototype results in length dimensions for openings in the model which produce purely laminar flow.

Numerous other engineering problems involve laminar flow through ducts having such short length-to-diameter ratios that a parabolic velocity profile cannot be established. For example, in recent designs of heat pumps and air-conditioning equipment (11), short capillary tubes have been used to replace more complicated two-way control valves. Also in the design of pneumatic instruments and compact heat exchangers or regenerators such entrance effects may be appreciable.

Object

The purpose of this investigation was as follows:

1 Determine experimentally the pressure drop characteristics (i.e., k) of capillary tubes having small length-to-diameter ratios.

2 To provide experimental data for laminar flow through tubes in the range of the dimensionless quantity $(L/D\mathrm{Re}_D)$ from 4×10^{-4} to that value of $(L/D\mathrm{Re}_D)$ where the Poiseuille law holds.

Apparatus and Experimental Procedure

A schematic flow diagram of the equipment used in this investigation is shown in Fig. 1. Compressed air from a large settling chamber passes through a needle valve, filter, and air drier to the test section. The test section consists of two 6-in-diam pipes between which a thin plate of aluminum or lucite is tightly clamped with rubber gaskets and flanges. At the inlet side, a baffle plate is installed in the pipe to dissipate the kinetic energy of the incoming stream.

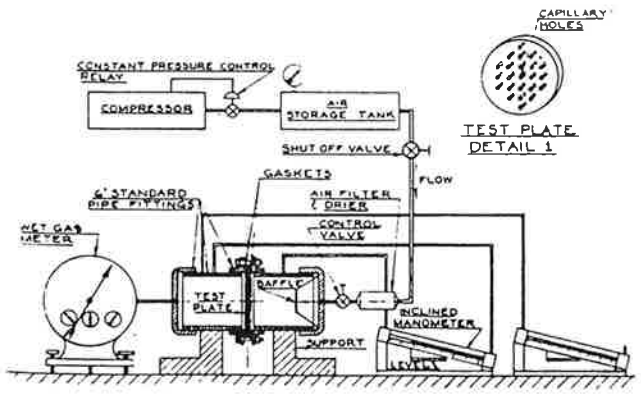

Fig. 1 Schematic Diagram of the Experimental Apparatus

Capillary holes of about $^1/_{32}$ or $^1/_{64}$ in. were drilled and reamed perpendicular to the face of the circular plate. The entrance and the exit of the holes were square-edged with sharp corners. Plate thickness of about $^1/_{64}$, $^1/_{32}$, $^1/_{16}$, $^1/_8$, $^1/_4$, and $^1/_2$ in. were used to obtain the desired length-to-hole diameter ratios.

It was decided to use several capillary holes in a parallel arrangement (see detail in Fig. 1) instead of a single hole, for two principal reasons: (*a*) The flow rate through a single capillary hole is exceedingly small and the available flowmeter would not have been suitable. (*b*) It is rather difficult to measure the diameter of a single capillary hole accurately and a larger number of holes offers a better means of obtaining a more reliable "average" size. It was arbitrarily decided to use 50 holes per plate. The holes were drilled about one or two thousandths of an inch undersize and then reamed to the final diameter. The size of the holes was measured by means of "go" and "no-go" gages, different in diameter by 0.001 in. Test data were reduced on the basis of a hole diameter halfway between the two gage diameters and, for purposes of evaluating the accuracy of the results, it was assumed that the diameter of an average hole was known to within 0.0005 in. on a 20:1 odd basis.

In order to ascertain whether or not the material or its roughness has an effect on the results, some of the earlier tests were first performed with the holes drilled in lucite plates and then repeated with aluminum plates. Since no effect could be observed only lucite plates were used in the later stages of the work because the transparent material permitted visual inspection of the holes.

To insure that there was no interference effect between the emerging air streams, check runs were made during which one half of the holes were plugged. It was found that the spacing of the holes had no effect on the results.

The principal data consisted of measurements of flow rate, pressure, and temperature in the downstream chamber of the test rig, and the differential pressure across the plate containing the capillary holes. The flow rate was measured by means of a stop watch and a vane-type wet flowmeter which had been calibrated carefully before the test program was initiated. The pressure and temperature on the downstream side of the holes were measured by means of an inclined manometer and a mercury-in-glass thermometer, respectively. The differential pressure (or the total pressure drop) was measured by means of an inclined manometer with a precision level.

Each test was repeated at least twice and the data were accepted only if the results agreed to within 3 per cent. Special care was taken at low flow rates where the differential-pressure measurements were the source of the largest potential uncertainty.

The pressure in the supply tank was not affected measurably by the outflow as would be expected from the small amount of air involved in any one test run. Therefore no pressure regulator was required.

Accuracy of Results

The accuracy of the experimental results was determined in accordance with a method suggested by Kline and McClintock (9) for single-sample experiments. Table 1 presents the percentage accuracy of the results in terms of uncertainty intervals based on 20-to-1 odds. This means that the odds are 20 to 1 against the per cent error in any one value of a result exceeding the stated percentage. The uncertainty intervals in the table are based on a combination of statistics and judgment, and they should be regarded as best estimates rather than absolute values. It is believed however that the accuracy of the final correlation of the data, represented by the curve drawn through all of the

experimental points (Fig. 5) is considerably better than the percentage figures for individual test points in Table 1.

TABLE 1 UNCERTAINTY INTERVAL FOR ANY ONE VALUE ON A 20-TO-1 ODDS BASIS

Result	Low differential pressure, 1/64 in. diam	Low differential pressure, 1/32 in. diam	High differential pressure, 1/64 in. diam	High differential pressure, 1/32 in. diam
$\overline{\Delta p}$	5	5	2	2
$\dot{Q}$	1/4	1/4	1/2	1/2
$\overline{\Delta p}/{}^1/_2\rho V^2$	11	8	8	5
$L/D\mathrm{Re}_D$	1/2	1/2	1	1

Results and Discussion

The test results are tabulated in Table 2 and are presented in Fig. 2 in the form of curves in which the flow rate per tube is plotted against the total pressure drop between the reservoirs. Each of the curves represents the data obtained in a series of tests with one particular test section (e.g., one capillary tube). Inspection of Fig. 2 shows that the curves for tubes of larger aspect ratios (L/D) have steeper slopes than those of smaller aspect ratios. The slope of each curve was measured and the results are plotted in Fig. 3 with the slope as ordinate and the aspect ratio as abscissa. The resulting curve shows that the exponent N in an equation of the type

$$\dot{Q} = \text{const } \overline{\Delta p}^N \quad [5]$$

increases from 0.5 at an aspect ratio approaching zero, to 0.91 at an aspect ratio of about 17. The exponent N in Equation [2] is related to k, the exponent of the velocity head in Equation [1] by

$$N = 1/2k \quad [6]$$

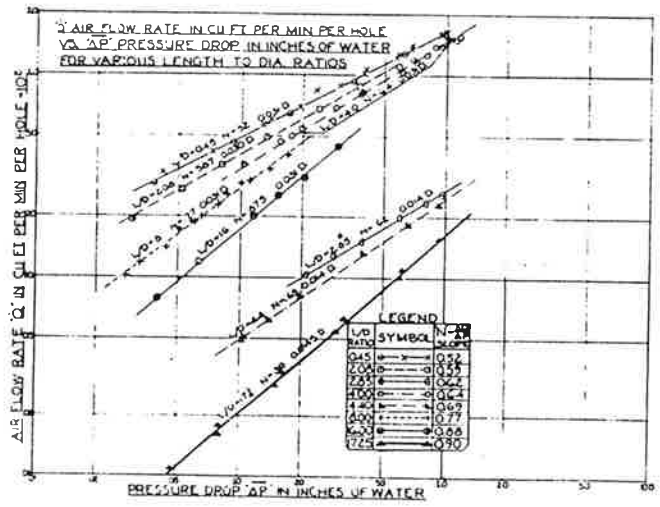

Fig. 2 Air Flow Rate Versus Pressure Drop in Capillary Tubes of Various Length-to-Diameter Ratios

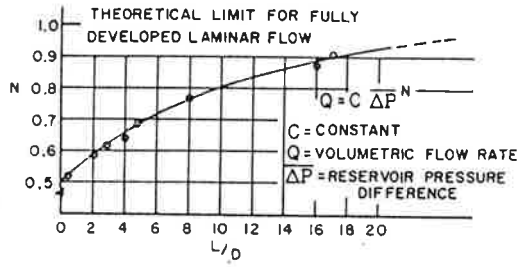

Fig. 3 Characteristic Flow Exponent N Versus Length-to-Diameter Ratio for Laminar Flow

Hence, the trend of the curve in Fig. 3 suggests an asymptotic approach to an exponent of unity, a value predicted from the Poiseuille law. The curve in Fig. 3 can be used to simulate, within the range of the variables shown in Fig. 2 and Table 2,

TABLE 2 EXPERIMENTAL DATA OF FLOW AND PRESSURE DROP IN SHORT CAPILLARY TUBES

$\overline{\Delta p}$ in. H_2O	$\dot{Q}$ cfm × 10^3	V fps	$\frac{L}{D}$	$\frac{\overline{\Delta p}}{\frac{1}{2\rho_c}\rho V^2}$	$\frac{L}{D\mathrm{Re}_D} \times 10^3$	Comments
0.091	0.465	14.60	0.45	1.92	1.97	Test rig 1
0.172	0.650	20.3	0.45	1.89	1.41	
0.35	0.938	29.3	0.45	1.84	0.99	
0.615	1.265	39.7	0.45	1.76	0.73	
0.073	0.435	13.6	0.45	1.78	2.12	Test rig 2
0.140	0.615	19.2	0.45	1.71	1.50	
0.136	0.622	19.5	0.45	1.63	1.47	
0.253	0.840	26.3	0.45	1.66	1.10	
0.40	1.070	33.5	0.45	1.61	0.86	
0.57	1.28	40.0	0.45	1.61	0.72	
0.67	1.40	43.9	0.45	1.58	0.656	
0.93	1.63	51.1	0.45	1.61	0.562	
0.042	0.333	10.4	0.45	1.75	2.76	Test rig 3
0.128	0.565	17.6	0.45	1.87	1.64	
0.193	0.697	21.85	0.45	1.825	1.32	
0.300	0.886	27.8	0.45	1.75	1.034	
0.391	1.020	31.9	0.45	1.735	0.90	
0.560	1.240	38.9	0.45	1.675	0.740	
0.672	1.355	42.4	0.45	1.68	0.68	
0.930	1.62	50.7	0.45	1.64	0.567	
0.975	1.66	52.0	0.45	1.635	0.560	
0.030	0.193	6.56	2.08	3.17	21.0	
0.081	0.360	12.25	2.08	1.45	11.3	
0.133	0.490	16.7	2.08	2.18	8.25	
0.052	0.272	9.25	2.08	2.75	15.1	
0.238	0.677	23.0	2.08	2.04	6.00	
0.376	0.880	30.0	2.08	1.89	4.60	
0.581	1.120	38.2	2.08	1.82	3.62	
0.21	0.104	16.1	2.85	3.62	25.2	
0.39	0.152	23.8	2.85	3.11	17.0	
0.60	0.200	31.8	2.85	2.51	12.7	
0.80	0.236	36.8	2.85	2.06	11.0	
0.96	0.260	40.4	2.85	2.67	10.0	
0.285	0.128	20.0	2.85	3.24	20.3	
0.102	0.381	11.3	4.0	3.63	22.7	Aluminum plate
0.155	0.475	14.9	4.0	3.18	17.3	
0.195	0.550	17.2	4.0	2.98	14.9	
0.286	0.702	22.0	4.0	2.67	11.7	
0.390	0.835	26.1	4.0	2.58	9.8	
0.595	1.06	33.0	4.0	2.44	7.7	
0.975	1.37	43.0	4.0	2.38	6.0	
0.020	0.118	3.7	4.0	6.67	70.0	
0.87	1.41	44.0	4.0	2.01	5.85	Lucite plate
0.68	1.21	38.0	4.0	2.14	6.75	
2.60	2.46	77.1	4.0	1.95	3.33	
1.50	1.82	59.1	4.0	1.94	4.35	
1.10	1.50	47.0	4.0	2.25	5.45	
1.15	1.56	49.0	4.0	2.17	5.30	
0.70	1.17	36.7	4.0	2.33	7.00	
0.93	1.42	44.5	4.0	2.10	5.76	
0.175	1.51	16.0	4.0	3.13	16.0	
0.38	0.82	25.8	4.0	2.57	9.9	
0.79	1.28	40.2	4.0	2.20	6.37	
0.96	1.45	45.5	4.0	2.10	5.64	
2.8	2.63	82.5	4.0	1.86	3.10	
4.5	3.40	108.0	4.0	1.75	2.38	
0.057	0.031	4.75	4.4	11.4	131.0	Lucite plate
0.105	0.051	7.9	4.4	7.7	79.0	
0.196	0.081	12.6	4.4	5.76	50.0	
0.396	0.132	20.5	4.4	4.25	30.7	
0.920	0.228	36.5	4.4	3.10	17.2	
0.655	0.184	28.5	4.4	3.63	22.0	
0.137	0.062	9.6	4.4	6.72	65.0	
0.102	0.049	7.6	4.4	8.00	82.1	
0.058	0.187	5.87	8.0	7.6	88.0	Lucite plate
0.100	0.289	9.05	8.0	5.63	57.6	
0.078	0.226	7.1	8.0	7.1	72.0	
0.044	0.139	4.36	8.0	10.5	119	
0.060	0.189	5.93	8.0	7.75	87.0	
0.065	0.199	6.05	8.0	8.1	85.0	
0.170	0.408	12.8	8.0	4.7	40	
0.028	0.101	3.16	8.0	12.7	103	
0.051	0.173	5.42	8.0	7.85	96.0	
0.086	0.256	7.7	8.0	6.61	66.5	
0.033	0.118	3.7	8.0	11.0	139	
0.110	0.298	9.35	8.0	5.7	54.7	
0.04	0.079	2.48	16.0	29.6	425	Lucite plate
0.085	0.160	4.96	16.0	15.6	206	
0.153	0.255	8.0	16.0	10.8	128	
0.293	0.421	13.2	16.0	7.65	77.8	
0.485	0.580	18.2	16.0	6.62	58.4	
0.06	0.119	3.7	16.0	20.9	277	
0.115	0.200	6.25	16.0	13.3	164	
0.205	0.313	9.8	16.0	9.65	105	
0.035	0.0073	1.06	17.25	142	2,250	Lucite plate
0.150	0.029	4.22	17.25	38.2	562	
0.295	0.054	7.85	17.25	21.6	302	
0.595	0.100	14.5	17.25	12.85	165	
0.99	0.149	21.6	17.25	9.58	110	
0.047	0.011	1.59	17.25	86.0	1,490	
0.160	0.034	4.95	17.25	29.5	480	
0.610	0.111	16.2	17.25	10.50	146	
0.935	0.156	22.7	17.25	8.25	105	
0.320	0.063	9.15	17.25	17.2	260	

various types of flow characteristics, since it is possible to obtain any value of k between 0.5 and 1.0 by a proper choice of the length-to-diameter ratio. The curve also shows that entrance effects can be appreciable in capillary tubes even at length-to-diameter ratios as large as 50.

The experimental data can also be correlated by means of an analysis originally proposed by Langhaar (1). The pressure drop between a reservoir and a downstream section in the tube x (Fig. 4) can be broken into three parts, or

$$\bar{p} - p_x = \Delta_1 p + \Delta_2 p + \Delta_3 p \quad \ldots\ldots\ldots\ldots [7]$$

where

$(\bar{p} - p_x)$ = drop between reservoir and a downstream section x
$\Delta_1 p$ = pressure drop between reservoir and inlet cross section ($x = 0$)
$\Delta_2 p$ = drop in pressure due to increase in kinetic energy in length x
$\Delta_3 p$ = pressure drop due to frictional loss in length x

If the stream tube between the reservoir and the section $x = 0$ is frictionless and has a bellmouth shape, the velocity at the inlet is approximately uniform (1, 7) and equal to the mean velocity V. Thus the pressure drop between the reservoir and the inlet section equals one velocity head according to Bernoulli's equation, or

$$\Delta_1 p = \frac{1}{2g_c} \rho V^2$$

Using the Navier-Stokes boundary-layer equations and Helmholtz's principle of least dissipation the remaining two pressure-drop terms, $\Delta_2 p$ and $\Delta_3 p$, have been evaluated by Langhaar (1) who showed that there exists for streamline flow in the transition length of tubes a unique relationship between $(\Delta_2 p + \Delta_3 p)$ and a single parameter $(x/D\mathrm{Re}_D)$. His results are shown graphically in Fig. 5 where

$$(\Delta_2 p + \Delta_3 p)/(\rho V^2/2g_c)$$

is plotted versus $(x/D\mathrm{Re}_D)$. The pressure-drop term $(\Delta_2 p + \Delta_3 p)$ also can be expressed in terms of a pipe-friction factor (8) by the equation

$$\frac{\Delta_2 p + \Delta_3 p}{\frac{1}{2g_c}\rho V^2} = \frac{p_0 - p_x}{\frac{1}{2g_c}\rho V^2} = 4 f_{APP} \frac{x}{D} = \phi\,(x/D\mathrm{Re}_D) \ldots [8]$$

where f_{APP} is an integrated apparent friction coefficient defined by Equation [8] and ϕ denotes a functional relation. The integrated apparent friction coefficient f_{APP} includes the effects of the viscous shearing stress as well as the change in velocity head or momentum flux caused by the change of the velocity profile between the inlet section ($x = 0$) and the section where p_x is measured.

With capillary tubes of the size used in this study it was not possible to obtain local static-pressure measurements. Instead, the pressure difference between the reservoirs upstream and downstream of the tubes were measured. To compare the experimental results with Langhaar's theory it was assumed that the static pressure at the outlet of the tube is equal to the downstream reservoir pressure (10). It was further assumed that as the fluid enters a tube it forms a stream tube having the shape of a bellmouth so that the assumptions regarding the term $\Delta_1 p$ are valid. Then the pressure difference between the reservoirs $\overline{\Delta p}$ is related to $p_0 - p_L$ by the relation

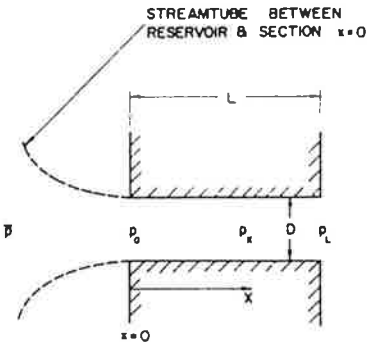

FIG. 4 SKETCH ILLUSTRATING NOMENCLATURE FOR TRANSITION FLOW

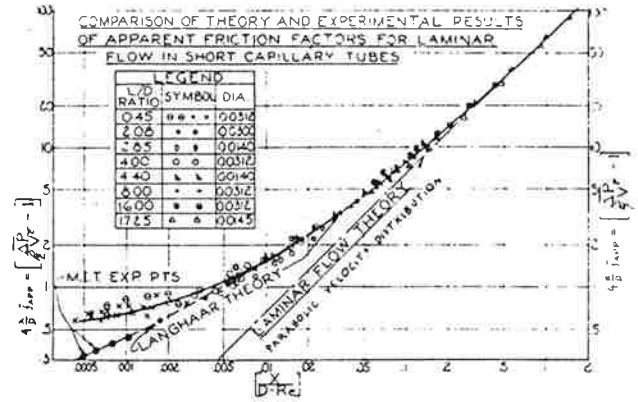

FIG. 5 COMPARISON BETWEEN THEORY AND EXPERIMENTAL RESULTS FOR LAMINAR FLOW IN SHORT CAPILLARY TUBES

$$\frac{\overline{\Delta p}}{\frac{1}{2g_c}\rho V^2} - 1 = \frac{p_0 - p_L}{\frac{1}{2g_c}\rho V^2} \quad \ldots\ldots\ldots\ldots [9]$$

The experimental results are shown in Fig. 5 where $\overline{\Delta p}/(\rho V^2/2g_c) - 1$ is the ordinate and $(L/D\mathrm{Re}_D)$ is the abscissa. Also shown on this graph are the analytical curve of reference (1), the Poiseuille relation for fully established laminar flow, and the averaged experimental results of reference (8). These experimental data were obtained with water and air in the entrance section of a 1.25-in-ID tube with a bellmouth entrance. The diameter Reynolds numbers Re_D used in reference (8) were large and resulted in turbulent flow downstream from the transition section.

Inspection of the data points and the curves of Fig. 5 shows that the experimental data for laminar flow in capillary tubes agree within the uncertainty interval (see Table 1) with the analysis of Langhaar (1) at values of the dimensionless quantity $(x/D\mathrm{Re}_D)$ greater than 4×10^{-3}, but deviate considerably at smaller values of $(x/D\mathrm{Re}_D)$. The test runs in this regime were repeated with three different test sections to verify the results.

The reason for the discrepancy between Langhaar's theory and the experimental results at $(x/D\mathrm{Re}_D)$ less than 4×10^{-3} can be found by examining the assumptions regarding $\Delta_1 p$. It was assumed that the stream tube formed by the fluid entering a tube has a bellmouth shape and that the velocity at the entrance section is uniform and equal to the average velocity V. However, even at very low Reynolds numbers small eddies form behind a sharp edge entrance and cause a vena contracta with some

friction losses. These losses, which are not considered in Langhaar's analysis, affect the over-all pressure drop appreciably when the tubes are so short that the total pressure drop between the reservoirs is of the order of one velocity head. Since the test data at $(x/D\mathrm{Re}_D)$ less than 4×10^{-3} were obtained in tubes having square-edged entrances and aspect ratios L/D of 0.45, the experimentally measured pressure losses are larger than those predicted by Langhaar's analysis. The geometry of these short tubes actually approaches that of an orifice for which the flow rate can be related by Torricelli's equation in the form

$$\dot{Q} = C \frac{\pi D^2}{48} \sqrt{\left(2g_c \frac{\overline{\Delta p}}{\rho}\right)} \quad [10]$$

The orifice coefficient C for the capillary tubes with an L/D ratio of 0.45 was found to be 0.76 ± 0.03 in the Reynolds-number range Re_D between 100 and 800. This result is in agreement with data obtained by Zucrow (12) in the same Reynolds-number range with benzol flowing through square-edged jets having an aspect ratio L/D of 0.33.

The experimental results obtained in the range of large values of $(x/D\mathrm{Re}_D)$ approach those predicted from the Poiseuille laminar-flow theory for a parabolic velocity distribution at values of $(x/D\mathrm{Re}_D)$ equal to 0.3.

Conclusions

From an experimental study of the flow characteristics of short capillary tubes the following conclusions can be drawn:

1 Measured values of the pressure drop between reservoirs upstream and downstream of capillary tubes with square-edged entrances are in agreement with Langhaar's theory for $(L/D\mathrm{Re}_D)$ larger than 4×10^{-3} and (L/D) larger than 2.

2 Measured values of the reservoir pressure drop for tubes having an aspect ratio L/D equal to 0.45 are considerably larger than those predicted by Langhaar's theory, but can be correlated by the usual orifice equation. The orifice coefficient for the range of Reynolds numbers Re_D between 100 and 800 was found to be 0.76 ± 0.03.

3 By proper selection of length-to-diameter ratios of short capillary tubes it is possible to simulate various flow characteristics in small-scale models for tests in atmospheric wind tunnels or in pneumatic control devices.

BIBLIOGRAPHY

1 "Steady Flow in the Transition Length of a Straight Tube," by H. L. Langhaar, *Journal of Applied Mechanics*, Trans. ASME, vol. 64, 1942, pp. A-55–58.

2 "Recherches expérimentales sur le movement des liquides dans les tubes de très petits diametres," by J. L. M. Poiseuille, *Memories des Savants Étrangers*, vol. 9, 1846, pp. 433–444.

3 "Hydrodynamique," by J. Boussinesq, *Comptes Rendus*, t. 110, 1890, pp. 1160, 1238; t. 113, 1891, pp. 9, 49.

4 "Die Entwicklung der Laminaren Geschwindigkeitsverteilung und ihre Bedeutung für Zähigkeitsmessungen," by L. Schiller, *Zeitschrift für angewandte Mathematik und Mechanik*, band 2, heft 2, 1922, pp. 96–106.

5 "Modern Developments in Fluid Dynamics," Fluid Motion Panel of the Aeronautical Research Committee, et al., edited by S. Goldstein, Clarendon Press, Oxford, England, 1938, pp. 304–308.

6 "Experimental Investigation of the Effects of Cooling on Friction and on Boundary Layer Transition for Low Speed Gas Flow at the Entry of a Tube," by S. J. Kline and A. H. Shapiro, NACA TN 3048, November, 1953.

7 "Applied Hydro- and Aeromechanics," by L. Prandtl and O. G. Tietjens, McGraw-Hill Book Company, Inc., New York, N. Y., first edition, 1934, pp. 27, 139–143.

8 "Friction Coefficients in the Inlet Length of Smooth Round Tubes," by A. H. Shapiro and R. Smith, NACA TN 1785, November, 1948.

9 "Describing Uncertainties in Single-Sample Experiments," by S. J. Kline and F. A. McClintock, *Mechanical Engineering*, vol. 75, 1953, pp. 3–8.

10 "The Dynamics and Thermodynamics of Compressible Fluid Flow," by A. H. Shapiro, Ronald Press, 1953.

11 "Capillary Tube Improves Heat Pump Design," by G. L. Biehn, *Heating and Ventilating*, vol. 51, no. 2, February, 1954, pp. 75–79.

12 "Discharge Characteristics of Submerged Jets," by M. J. Zucrow, Bulletin No. 31, Purdue Engineering Experiment Station, 1928.

Discussion

M. A. Rivas, Jr.[5] The experimental data presented in the paper are quite valuable due, in particular, to the care taken by the authors in their experiments. However, the writer takes exception to the lack of emphasis on what constitutes the governing design parameter for laminar flow in tubes (or capillaries). As has been shown by theoretical and experimental investigations (the authors' references (1), (3), (4), (5), and reference[6] of this discussion), the sole parameter which governs the flow is $L/D/\mathrm{Re}_D$ or $\mathrm{Re}_x/\mathrm{Re}_D$[2].

In particular, the writer is disturbed by the correlation presented in Fig. 3 of the paper where the exponent N in equation [5]

$$\dot{Q} = \text{const.}\ \overline{\Delta p}^N \quad [5]$$

is depicted as a function of L/D alone. It will be shown that it is legitimate to write an expression as given by Equation [5], but that N, however, in this expression is a function of $L/D/\mathrm{Re}_D$ and not of L/D.

It is easily shown (e.g., from Equations [8] and [9]) that the total pressure drop between the two reservoirs (assuming that, as the fluid enters the tube, it forms a stream tube having the shape of a bellmouth—for a detailed discussion of flow on bellmouth entries (see reference[7] of this discussion) is given by

$$\overline{\Delta P} = \left(1 + 4\bar{f}_{\mathrm{APP}} \frac{x}{D}\right) \frac{1}{2} \rho V^2 \quad [11]$$

or

$$\overline{\Delta P} = \left(1 + 4\bar{f}_{\mathrm{APP}} \frac{x}{D}\right) \frac{1}{2} \rho \left(\frac{Q}{A}\right)^2 \quad [11a]$$

transposing

$$Q = \frac{A}{\sqrt{(\rho/2)}} \frac{\overline{\Delta P}^{1/2}}{\sqrt{(1 + 4\bar{f}_{\mathrm{APP}} x/D)}} \quad [12]$$

For laminar flow in tubes (see Figs. 4 and 5 in reference[6] or Fig. 5 of the paper),

(a) If $(x/D)/\mathrm{Re}_D$ is very small $< 10^{-5}$

then

$$4\bar{f}_{\mathrm{APP}} \frac{x}{D} << 1$$

and therefore, from Equation [12]

---

[5] First Lieutenant, USAF, Directorate of Research, Fluid Dynamics Research Branch, Aeronautical Research Laboratory, Wright Air Development Center, Air Research and Development Command, Wright-Patterson Air Force Base, Ohio. Assoc. Mem. ASME.

[6] "Friction Factor in the Laminar Entry Region of a Smooth Tube," by A. H. Shapiro, Robert Siegel, and S. J. Kline, Proceedings of the Second U. S. National Congress of Applied Mechanics, June, 1954, pp. 733–741.

[7] "On the Theory of Discharge Coefficients for Rounded-Entrance Flowmeters and Venturies," by M. A. Rivas, Jr. and A. H. Shapiro, Trans. ASME, vol. 78, 1956, pp. 489–498.

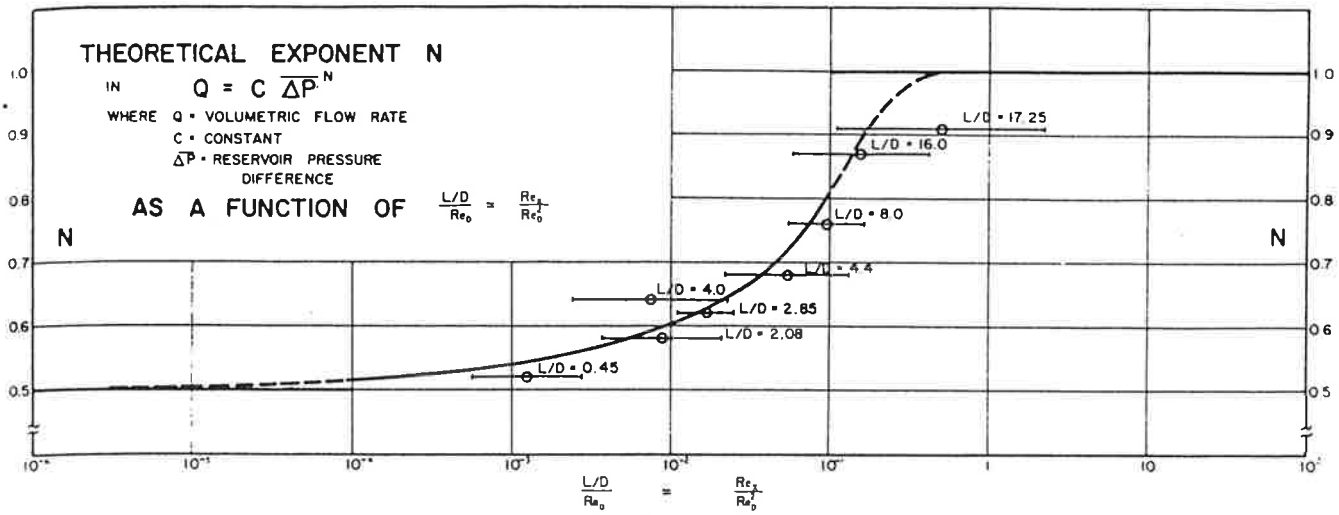

FIG. 6

$$Q \sim \overline{\Delta P}^{1/2}; \quad N = 1/2$$

The same result is obtained if $4\bar{f}_{APP}(x/D)$ is constant.

(*b*) If $(x/D)/\mathrm{Re}_D$ is high >0.5

then

$$4\bar{f}_{APP}\,\frac{x}{D} \gg 1$$

and therefore, from Equation [12]

$$Q \sim \frac{\overline{\Delta P}^{1/2}}{\sqrt{\left(4\bar{f}_{APP}\,\frac{x}{D}\right)}}$$

but since, in this range

$$4\bar{f}_{APP}\,\frac{x}{D} = \frac{64\,\frac{x}{D}}{\mathrm{Re}_D} \sim \frac{1}{V} \sim \frac{1}{Q}$$

we then have

$$Q \sim \frac{\overline{\Delta P}^{1/2}}{\frac{1}{\overline{Q}^{1/2}}} \quad \text{or} \quad Q \sim \overline{\Delta P}; \quad N = 1$$

(*c*) If $10^{-5} < \dfrac{x}{D}\Big/\mathrm{Re}_D < 0.5$

$$Q \sim \frac{\overline{\Delta P}^{1/2}}{\sqrt{\left(1 + 4\bar{f}_{APP}\,\frac{x}{D}\right)}}$$

but since

$$4\bar{f}_{APP}\,\frac{x}{D} = \varphi_1\left(\frac{\frac{x}{D}}{\mathrm{Re}_D}\right)$$

also

$$1 + 4\bar{f}_{APP}\,\frac{x}{D} = \varphi_2\left(\frac{\frac{x}{D}}{\mathrm{Re}_D}\right)$$

In particular we could define an exponent n such that

$$1 + 4\bar{f}_{APP}\,\frac{x}{D} \sim \left(\frac{\frac{x}{D}}{\mathrm{Re}_D}\right)^n \qquad [13]$$

or

$$1 + 4\bar{f}_{APP}\,\frac{x}{D} \sim \left(\frac{1}{Q}\right)^n \qquad [13a]$$

Substituting Expression [13*a*] into [12]

$$Q \sim \frac{\overline{\Delta P}^{1/2}}{\left(\frac{1}{Q}\right)^{n/2}} \qquad [14]$$

or

$$Q \sim \overline{\Delta P}^{\frac{1/2}{1-n/2}} = \overline{\Delta P}^{N} \qquad [15]$$

where

$$N = \frac{1/2}{1 - n/2} \qquad [16]$$

The exponent n can be calculated readily from the curve given in Fig. 5 of the authors' paper; however, the curve in Fig. 5 in reference[6] has been used instead, since it is in a form that yields a greater accuracy. Having calculated n, N is readily computed from Equation [16]. The results of these calculations are presented in Fig. 6.

The apparently successful correlation given by the authors in their Fig. 3 is explained as follows: If, from the authors' Table 2 and from their Fig. 3, we construct Table 3 and plot these data on Fig. 6 in the manner shown, where each solid horizontal line represents for each L/D the range of $(L/D)/\mathrm{Re}_D$ at its corresponding N-value, and each circle represents the mean value of the $(L/D)/\mathrm{Re}_D$ range, we can see how the authors were able to arrive at the smooth correlation shown in their Fig. 3. Therefore, it was quite

TABLE 3

L/D	Range of $L/D/\mathrm{Re}_D$		N
0.45	2.76×10^{-3}	5.60×10^{-4}	0.52
2.08	2.1×10^{-2}	3.62×10^{-3}	0.58
2.85	2.52×10^{-2}	1.1×10^{-2}	0.62
4.0	2.27×10^{-2}	2.38×10^{-3}	0.64
4.4	1.31×10^{-1}	2.2×10^{-2}	0.68
8.0	1.63×10^{-1}	5.47×10^{-2}	0.76
16.0	4.25×10^{-1}	5.8×10^{-2}	0.87
17.25	2.25	1.1×10^{-1}	0.91

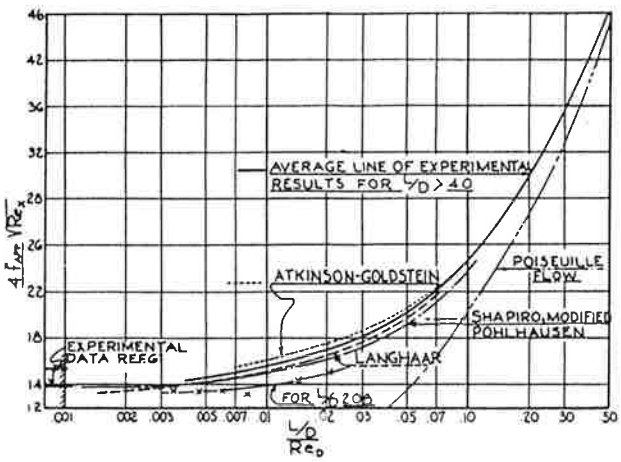

FIG. 8 COMPARISON OF THEORETICAL AND EXPERIMENTAL RESULTS FOR INTEGRATED APPARENT FRICTION FACTOR

by L/D variations even when L/D is of the order of 0.1. The ISA and ASME codes specify the maximum thickness of orifice plates, t, as a fraction of the pipe diameter, D_p; i.e., $t < 0.02\ D_p$. For a small orifice in a large pipe it is therefore quite possible that the pressure drop through the orifice, although designed according to specifications, will deviate from the results predicted from a simple orifice equation (e.g., footnote 8). To safeguard against such deviations it is suggested that the maximum orifice thickness be specified in terms of the orifice diameter.

The information available to date is unfortunately insufficient to give quantitative answers to the questions raised by Professor Shapiro's valuable and pertinent comments which, however, are broader in scope than the limited objectives for which the tests reported in this paper were conducted. Qualitatively, we can conclude that only for conditions when $\Delta_1 p$ in Equation [7] is of the order of $(\Delta_2 p + \Delta_3 p)$ will deviations from the pressure drop predicted from Equation [9] and Fig. 5 be appreciable.

The authors agree with Lieut. Rivas and Professor Shapiro that additional experiments, especially at Reynolds numbers between 500 and 2100 and in the low L/D range, are desirable. The tests reported by the authors were conducted within the scope of a large research project in the course of which experimental data for flow of air through capillary tubes in the pressure-drop range of 0.03 and 2.0 in. water were required. These conditions yield $(L/D)/\mathrm{Re}_D$ values between 1×10^{-3}, the maximum value for which data were available and 0.5, the value at which Poiseuille flow is approached. The data were published simply because they fall into a range of variables in which no experimental results were heretofore available. When comparing the accuracy of the experimental results of this study with those of Shapiro, et al.,[6] it is well to keep in mind that the pressure drop, which more than any other measurement limits the accuracy of the apparent friction coefficient at low Reynolds numbers, is much smaller in the range of variables covered by the authors than in the range of variables covered by Shapiro, et al. The original equipment was returned to the sponsor at the termination of the contract, but an improved version is at present being built at Union College to conduct further tests along the lines suggested by the discussers.

Dean Smith's comments regarding the units and the dimensional treatment of the subject seem to have been prompted by an error in the preprint of this paper, where instead of the proportional sign an equal sign was used in Equation [1]. Equation [1] is dimensionally consistent as shown and the parameters $\Delta p/(\rho\ V^2/2g_c)$ and $(L/D\mathrm{Re}_D)$ are dimensionless quantities. One could, of course, express ρ in slugs/ft^3 instead of lb$_M$/ft^3 and thereby eliminate the explicit use of g_c. This choice of units may be more satisfactory to some, but it would not affect the mathematical rigor.

Mr. Sproats comments on the application of capillary tubes to flow measurements will be of value to those contemplating the use of capillaries for this purpose. It would seem, however, that the minimum length should be specified in terms of $(L/D)/\mathrm{Re}_D$ instead of L/D. The experimental results of this study confirm theoretical predictions[6] which show that for the centerline velocity to approach the Poiseuille value within 1 per cent, $(L/D)/\mathrm{Re}_D$ must be at least 0.3, but probably close to 0.6. With the lower figure as a limit, the minimum length-to-diameter ratio required to establish a parabolic velocity profile at Re_D of 2000 is 600, which is twelve times larger than the value suggested by Mr. Sproats.